Optical Observations of the Binary Pulsar System PSR B1718−19: Implications for Tidal Circularization

M. H. van Kerkwijk[1,2], V. M. Kaspi[3], A. R. Klemola[4], S. R. Kulkarni[5], A. G. Lyne[6], and D. Van Buren[7]

ABSTRACT

We report on Keck and *Hubble Space Telescope* optical observations of the eclipsing binary pulsar system PSR B1718−19, in the direction of the globular cluster NGC 6342. These reveal a faint star ($m_{\rm F702W} = 25.21 \pm 0.07$; Vega system) within the pulsar's $0\farcs5$ radius positional error circle. This may be the companion. If it is a main-sequence star in the cluster, it has radius $R_{\rm C} \simeq 0.3\,R_\odot$, temperature $T_{\rm eff} \simeq 3600\,{\rm K}$, and mass $M_{\rm C} \simeq 0.3\,M_\odot$. In many formation models, however, the pulsar (spun up by accretion or newly formed) and its companion are initially in an eccentric orbit. If so, for tidal circularization to have produced the present-day highly circular orbit, a large stellar radius is required, i.e., the star must be bloated. Using constraints on the radius and temperature from the Roche and Hayashi limits, we infer from our observations that $R_{\rm C} \lesssim 0.44\,R_\odot$ and $T_{\rm eff} \gtrsim 3300\,{\rm K}$. Even for the largest radii, the required efficiency of tidal dissipation is larger than expected for some prescriptions.

Subject headings: binaries: close — pulsars: individual (PSR B1718−19) — stars: evolution

[1]Astronomical Institute, Utrecht University, P. O. Box 80000, 3508 TA Utrecht, The Netherlands; M.H.vanKerkwijk@astro.uu.nl

[2]Institute of Astronomy, University of Cambridge, Madingley Road, Cambridge, CB3 0HA, UK

[3]Massachusetts Institute of Technology, Physics Department, Center for Space Research 37-621, 70 Vassar Street, Cambridge, MA 02139; vicky@space.mit.edu

[4]UCO/Lick Observatory, University of California, Santa Cruz, CA 95064; klemola@ucolick.org

[5]Palomar Observatory, California Institute of Technology 105-24, Pasadena, CA 91125, USA; srk@astro.caltech.edu

[6]Department of Physics, University of Manchester, Jodrell Bank, Macclesfield, SK11 9DL, UK; agl@jb.man.ac.uk

[7]Infrared Processing and Analysis Center, California Institute of Technology, Pasadena, CA 91125; dave@ipac.caltech.edu

1. Introduction

PSR B1718−19 is a 1-s radio pulsar in the direction of the globular cluster NGC 6342 (Lyne et al. 1993). It is in a 6.2 h circular binary orbit with a companion that has mass $M_{\rm C} \geq 0.11\,M_\odot$ (assuming a pulsar mass $M_{\rm PSR} \simeq 1.35\,M_\odot$). At radio frequencies around 400–600 MHz, irregular eclipses of the pulsar occur around superior conjunction, indicating the presence of material around the companion. The eclipsing material must be tenuous since the eclipses are absent at higher frequencies. The properties of the pulsar itself are not special; from the spin period and its derivative, one infers a dipole magnetic field strength $B \simeq 3.2\times10^{19}(P\dot{P})^{1/2} \simeq 1.5\times10^{12}$ G and a spin-down age $\tau_{\rm sd} = P/2\dot{P} = 10$ Myr.

The system appears peculiar for several reasons (Lyne et al. 1993): (i) supernova activity in NGC 6342 should have ceased long ago, hence one does not expect it to contain an apparently recently formed pulsar; (ii) all other known binary pulsars in globular clusters have millisecond periods and low magnetic fields, evidence that they were "recycled" or spun up by accretion from a binary companion, the field presumably having decayed in the process (for a review, see Van den Heuvel 1995); (iii) unlike in other eclipsing pulsars, the rotational energy loss of PSR B1718−19 is many orders of magnitude below the critical flux necessary to drive a wind from the companion, so the origin of the eclipsing material is unclear.

Earlier papers on this system (Lyne et al. 1993; Ergma 1993; Wijers & Paczynski 1993; Zwitter 1993; Burderi & King 1994; Ergma, Sarna, & Giersz 1996) have focused on the three peculiarities discussed above, mostly in the context of the two favored formation scenarios: forming a new pulsar by accretion-induced collapse of a white dwarf, and recycling an old pulsar in a close encounter with other stars in the core of the globular cluster. We believe, however, another important issue is that (iv) the current orbit is near-circular ($e \lesssim 0.005$), while the formation should have left the pulsar and its companion in an eccentric orbit. An initially eccentric orbit is not only expected in all formation models, but also indicated by the fact that the system currently is not in the core of the cluster, as would be expected given its mass, but offset by $2\farcm4$; apparently, it received a kick, which should have made the orbit eccentric as well.

It has been noted by Verbunt (1994) that if circularization occurred, the energy dissipated in the companion would have been of order the binding energy of the star. Thus, the star might have become bloated or even have been partially destroyed. Little attention, however, has been given to the question of whether the tidal circularization efficiency is sufficient for circularization to have happened within the spin-down age.

The above puzzles motivated us to try to identify the counterpart of PSR B1718−19. In this article, we report on Jodrell Bank, Very Large Array (VLA), Keck and *Hubble Space Telescope* (*HST*) observations of PSR B1718−19. The improved position of the pulsar from the radio observations and the results of the optical imaging observations are reported and summarized in § 2. Given the crowded field, establishing a precise tie between the radio and optical observations is crucial. A detailed account of our astrometry is given in § 3. The photometry of a candidate object is also reported in this section. The constraints on the basic parameters of the companion derived from optical and pulsar timing observations are discussed in § 4. In § 5, we discuss the implications of our results, focusing in particular on the circularization.

2. Observations

The position of the pulsar was first determined from radio timing measurements using the 76-m Lovell telescope at Jodrell Bank (Lyne et al. 1993). We derived an improved timing position from data obtained between 1994.6 and 1998.8: $\alpha_{\rm J2000} = 17^{\rm h}21^{\rm m}01\fs53$ and $\delta_{\rm J2000} = -19\degr36\arcmin36\farcs$, with uncertainties of $0\fs04$ and $6\farcs$, respectively. This position has a relatively large uncertainty in declination because of the source's proximity to the plane of the ecliptic. An image of the field was obtained on 11 November 1992 using the VLA in the A-configuration. It reveals a source within the timing error box with a flux density of 0.3 mJy, consistent with the flux of the pulsar at the observing frequency of around 1400 MHz. The position of this source is $\alpha_{\rm J2000} = 17^{\rm h}21^{\rm m}01\fs54$ and $\delta_{\rm J2000} = -19\degr36\arcmin36\farcs6$, with an uncertainty of $0\farcs2$ in each coordinate.

The PSR B1718−19 field was observed on 4 June 1995 using the Low-Resolution Imaging Spectrometer (LRIS; Oke et al. 1995) on the 10-m Keck telescope. Two series of exposures with integration times ranging from 10 s to 240 s were taken through several filters. The seeing was $\sim 0\farcs9$ during the first series,

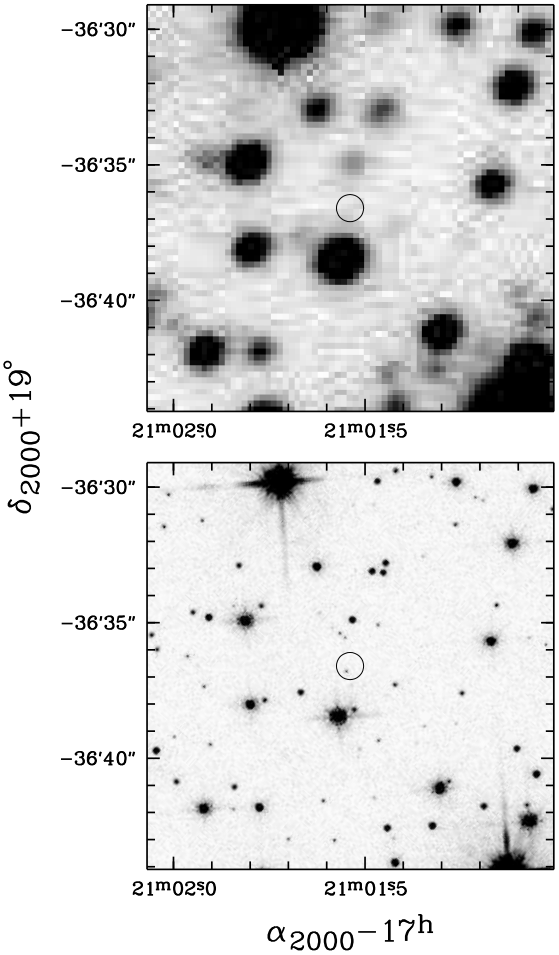

Fig. 1.— Optical images of the field of PSR B1718−19. The top panel shows part of the LRIS I-band image. The exposure time was 240 s and the seeing 0.″9. The limit to the flux of any star within the 0.″5 radius (95% confidence) error circle centered on the VLA position is $I > 24.0$ (95% confidence). The bottom panel shows part of the Planetary Camera image, taken through the the F702W filter. The image shown is the median of all twelve 700 s exposures. The candidate counterpart has $m_{\rm F702W} = 25.21 \pm 0.07$.

and $\sim$1.″2 during the second. Our best-seeing I-band ($\sim 0.8\mu m$) image is shown in Fig. 1. These images showed that there was no object in the VLA error box, and that with 95% confidence $I > 24.0$ mag. Furthermore, they showed that a brighter star was so close that it would be hard to make any further progress from the ground.

The Wide Field Planetary Camera 2 (WFPC2) on board the *HST* was used to observe the field through the F702W filter in four contiguous *HST* orbits, from 14:39 to 20:07 UT on 8 March 1997. In each spacecraft orbit, three 700-s exposures were taken, offset in both X and Y by 0, 3, and 6 PC pixels in order to mitigate the effects of hot pixels and imperfect flat fields. The pointing was such that the field around the pulsar is on a clean spot on the CCD of the Planetary Camera (PC).

The reduction and analysis started from the pipeline-calibrated PC images (Holtzman et al. 1995a). We first obtained median images for each of the three observing positions. The median image for the middle offset was used for the astrometry described below. Next, for each of the three sets, we found pixels hit by cosmic rays in the individual images by comparison with the median image; pixels with values more than 5σ above the median were replaced with the median (here, σ is an estimate of the expected uncertainty based on the median value). Finally, the images were registered by applying integer pixel shifts and co-added to form a grand average. This average is free of cosmic rays, but not of hot pixels and other chip defects. We used it for the photometry nonetheless, as our candidate (see below) and the other stars we selected were on clean parts of the chip. For display purposes, however, we have used the median of all registered images in Fig. 1.

3. Astrometry and Photometry

The astrometry of the PSR B1718−19 field was carried out in four stages. First, 23 stars from the ACT Reference Catalog (Urban, Corbin, & Wycoff 1998b) were used to derive an astrometric solution for a plate taken at epoch 1988.37 on Kodak 103a-G emulsion using the yellow lens of the 0.5-m Carnegie double astrograph at Lick Observatory. The model employed five terms in each coordinate (proportional to 1, x, y, xy, and (x^2, y^2) in (x, y)). The inferred rms error for a single star is 0.″16 in each coordinate, and the zero-point uncertainty in the solution 0.″04. We note that the errors are larger by about 50% than expected based on the measurement and ACT coordinate uncertainties. Probably, this is because some stars are blended with fainter objects; thus, it should induce no systematic error.

Second, the plate solution was used to calculate right ascension and declination for 30 fainter, rela-

tively isolated stars in common with the short LRIS R-band exposure. For these stars, positions were also measured on the LRIS frame, and corrected for instrumental distortion using a bi-cubic transformation determined by J. Cohen (1997, private communication). Solving for offset, scale and rotation, the inferred rms single-star error is $0\farcs26$ in each coordinate, consistent with the expected measurement errors on the astrograph plate for these relatively faint stars. The zero-point uncertainty in the solution is $0\farcs05$.

Third, using 23 fainter stars on a smaller part of the LRIS image around the VLA position of PSR B1718−19, the solution was transferred to one of the 240 s LRIS R-band images, solving only for the offset between the two exposures. The inferred rms error is $0\farcs011$ in each coordinate, and the zero-point uncertainty in the solution $0\farcs002$.

Finally, 37 stars were used to tie the astrometry to the WFPC2 PC image (14 of these were used in the previous stage as well). The WFPC2 positions were corrected for instrumental distortion using the cubic transformation given by Holtzman et al. (1995a). Offset, scale and rotation were left free in the solution[8]. The inferred rms error was $0\farcs017$ in each coordinate, and the zero-point uncertainty in the solution $0\farcs003$.

From the numbers above, the total uncertainty in the zero points of positions due to measurement errors is $0\farcs06$ in each coordinate. We expect systematic effects to be smaller than this; e.g., no large systematic offset as a function of magnitude is seen on yellow astrograph plates used for other applications. A possible additional uncertainty is the extent to which our ACT-based solution is on the same system as the VLA position of PSR B1718−19, i.e., the International Celestial Reference System (ICRS). The ACT combines the Tycho (ESA 1997) and AC2000 (Urban et al. 1998a) catalogs to determine positions and accurate proper motions. The Tycho positions are on the ICRS to within 0.6 mas (ESA 1997), and any offset from the ICRS at the plate epoch, which is close to the Tycho epoch (1991.25), should be small as well.

In summary, we expect the uncertainties in the astrometry to be dominated by measurement errors, $0\farcs06$ in each coordinate for the optical position, and $0\farcs2$ for the radio position. Combining the two in quadrature, the 95% confidence error radius is $[-2\log(1-0.95)(0\farcs2^2+0\farcs06^2)]^{1/2} = 0\farcs5$. Within this radius, there is one faint object (Fig. 1), at $\alpha_{\rm J2000} = 17^{\rm h}21^{\rm m}01\fs549 \pm 0\fs004$ and $\delta_{\rm J2000} = -19^\circ36'36\farcs76 \pm 0\farcs06$. This may be the optical counterpart of PSR B1718−19.

We measured magnitudes for the candidate counterpart of PSR B1718−19 and for a number of other stars in the field following the prescriptions of Holtzman et al. (1995b) and Baggett et al. (1997). We performed aperture photometry for a range of different radii, and used some thirty brighter stars in the frame to determine aperture corrections relative to the standard $0\farcs5$ (11 pix) radius aperture. For the candidate, the best signal-to-noise ratio is for relatively small apertures, with radii between 1.5 and 3 pix. From these, we infer a count rate for the $0\farcs5$ radius aperture of $0.070 \pm 0.005\,{\rm DN\,s^{-1}}$ (we find consistent values for the larger apertures; here, 1 DN corresponds to about 7 electrons, given the gain used for our observations). This count rate corresponds to a magnitude $m_{\rm F702W} = 25.21 \pm 0.07$ in the Vega system (using $m_{\rm F702W} = 22.428$ for a count rate of $1\,{\rm DN\,s^{-1}}$ in the PC, and applying a 0.10 mag aperture correction from $0\farcs5$ radius to "nominal infinity"; Baggett et al. 1997). Magnitudes for the individual frames show a standard deviation of 0.25 mag around the average, similar to what is found for other stars at this brightness level. We do not find modulation at the $6\fh2$ orbital period of PSR B1718−19 (which is well covered by our observations), although the limit on the modulation amplitude is not very restrictive: < 0.3 mag at 95% confidence.

At or above the brightness level of the candidate counterpart, there is about one object per four square arcseconds in this field. Thus, there is a probability of about one in five of finding an object within the 95% confidence error radius by chance. If it is a chance coincidence, the real counterpart must be substantially fainter. We derive a 95% confidence limit of $m_{\rm F702W} = 27.2$ for any other object in the error circle (using the observed noise in the sky near the VLA position, of $\sigma_{\rm sky} = 5.6 \times 10^{-4}\,{\rm DN\,pix^{-1}\,s^{-1}}$, and the fact that within the $0\farcs5$ radius error circle there are about 400 resolution elements).

[8]The fitted scale is close to the value given by Holtzman et al. (1995a), as is the offset between the fitted position angle and the position angle of the *HST* V3 axis listed in the image header. If we fix the values, the inferred position of our proposed counterpart changes by $0\farcs006$ in RA and $-0\farcs005$ in Dec. Thus, a perhaps more conservative estimate of the zero-point uncertainty is about $0\farcs01$ in each coordinate.

4. Observational Constraints

We now evaluate the constraints set on the system by the observations. We first summarize the constraints on the age of the system and the mass of the companion set by radio observations, and then discuss the constraints on the companion radius and temperature from our *HST* detection and Keck limit. We will assume that we detected the companion, and that the system is located in NGC 6342.

4.1. System Age

Clearly, something happened to the system recently (as compared to the cluster age). One indication is the short inferred spin-down age of the pulsar, $\tau_{\rm sd} = P/2\dot{P} = 10\,{\rm Myr}$. This is the time required for a dipole rotating *in vacuo* to spin down to the present-day spin period from an infinitely fast rotation rate. It is thus an upper limit to the true age, unless other mechanisms influenced the spin period (e.g., transient spin-up by accretion or a braking index very different from that predicted by dipole emission).

Another indication of a recent event is that the system is offset from the cluster core. Unperturbed, a system as massive as this should have settled in the core long ago due to mass segregation (in $\sim 0.5\,{\rm Gyr}$ given its present position). Indeed, the progenitor(s) of this system, which must have been massive as well, should have resided in the core. It seems natural to argue that it was a single event that brought the system to its present state and kicked it out of the core.

We note that it would require fine-tuning for the kick to have resulted in the system remaining in a cluster orbit as wide as is indicated by the $2\farcm4$ offset (the half-mass radius is $0\farcm9$; for a discussion, see, e.g., Phinney 1992). If instead the system is unbound, the kick needs to have happened $\lesssim 1\,{\rm Myr}$ ago, which would imply that the event left the pulsar with a spin period only slightly shorter than the present one. This would be consistent with scenarios in which the pulsar was spun up by accretion: for Eddington-limited accretion, the equilibrium spin period is close to 1 s (Lyne et al. 1993). We conclude that the system has been in its present state for 10 Myr at most.

4.2. Companion Mass

Radio pulse timing of PSR B1718−19 has yielded the mass function, $f(M_{\rm C}, M_{\rm PSR}) = M_{\rm C}^3 \sin^3 i/(M_{\rm C} + M_{\rm PSR})^2 = 0.000706\,M_\odot$, where i is the inclination of the binary orbit (Lyne et al. 1993). From the mass function, assuming $M_{\rm PSR} \simeq 1.35\,M_\odot$ (Thorsett & Chakrabarty 1999), one infers $M_{\rm C} \geq 0.11\,M_\odot$; furthermore, there is a 95% *a priori* probability that $i > 18^\circ$ and hence that $M_{\rm C} < 0.43\,M_\odot$.

The radio eclipses allow a direct constraint on i, albeit in a model-dependent way. Burderi & King (1994) and Thorsett (1995) calculated the expected attenuation of the radio flux at different frequencies for a simple constant-velocity, spherically symmetric wind, and found that they could reproduce the observations of Lyne et al. (1993) for $i \gtrsim 30^\circ$. This would correspond to $M_{\rm C} \lesssim 0.25\,M_\odot$. Burderi & King argue that almost certainly $i > 20^\circ$, implying $M_{\rm C} < 0.35\,M_\odot$. In summary, most likely $0.11 \lesssim M_{\rm C} \lesssim 0.35\,M_\odot$.

4.3. Companion Radius and Temperature

The interpretation of the apparent F702W magnitude depends on the companion radius $R_{\rm C}$, effective temperature $T_{\rm eff}$, and (to a lesser extent) surface gravity $\log g$, as well as the distance and reddening to NGC 6342. To determine the constraint set by our measurement, we used parameters for NGC 6342 from the May 1997 edition of the catalog of globular clusters (Harris 1996): reddening $E_{B-V} = 0.44$, distance modulus $(m-M)_V = 16.15$, and metallicity relative to solar [Fe/H] $= -0.65$. The distance scale used in the catalog is similar to the Hipparcos-based one (e.g., that of Chaboyer et al. [1998] would give $(m-M)_V = 16.22$). The reddening corresponds to $A_V = 1.36$, $A_R = 1.02$, $A_I = 0.65$ (using the extinction curve of Mathis 1990), and one infers $(m-M)_0 = 14.79$ and $d = 9.1\,{\rm kpc}$. We also used the evolutionary tracks for [Fe/H] $= -0.5$ stars of Baraffe et al. (1998), to relate temperatures and radii to absolute magnitudes in various standard bands.

With these data in hand, we proceeded as follows. First, we looked up temperatures and corresponding radii for the main sequence (at age 10 Gyr, appropriate for a metal-rich globular cluster; Salaris & Weiss 1998). Second, we used M_V and M_R for these stars to calculate $V_{\rm ms}$ and $R_{\rm ms}$ for the distance and reddening of NGC 6342. Third, for each $(V-R)_{\rm ms}$, we used the calibration of Holtzman et al. (1995b; Eq. 9, Table 10) to infer the expected $R_{\rm F702W}$ magnitude corresponding to the observed F702W count rate. Fourth, we derived the radii required to match the observations from the difference $R_{\rm F702W} - R_{\rm ms}$. To estimate the uncertainty, we assumed a total uncer-

tainty of 0.3 mag in the magnitude difference, which we regard as a 95% confidence estimate (it is dominated by the estimated uncertainties in distance and reddening). Strictly speaking, one should redden the F702W magnitude and then calculate $R_{\rm F702W}$ using $(V-R)_0$. Furthermore, one should consider the influence of $\log g$ on the star's colors, and take into account the slight difference in metallicity. None of these corrections, however, is important at the present level of accuracy.

Another constraint is set by our I-band nondetection. This corresponds to an upper limit to the $m_{\rm F702W} - I$ color, and thus a lower limit to the effective temperature. We find $T_{\rm eff} > 3150\,{\rm K}$ for $m_{\rm F702W} - I > 1.4$ (here, we have decreased the limit to the magnitude difference by 0.2 mag to account for uncertainties in $m_{\rm F702W}$, in the color transformation, in the effects of changes in $\log g$, and in the reddening).

The observational constraints can be summarized graphically in a diagram of $R_{\rm C}$ versus the effective temperature $T_{\rm eff}$ of the companion (see Fig. 2). To make further progress we need to have some knowledge of the companion's nature. We consider two cases: the companion is an ordinary main sequence star; and the companion is a bloated star.

4.3.1. A Main Sequence Companion

In Fig. 2, the locus of radius versus effective temperature for main sequence stars of different masses is indicated (from Baraffe et al. 1998). From the intersection with the region allowed by our observation, one infers that if the companion were a main sequence star, it would need to have $0.26 \lesssim R_{\rm C} \lesssim 0.33\,R_\odot$ and $3580 \lesssim T_{\rm eff} \lesssim 3680\,{\rm K}$. Its mass would be $0.26 \lesssim M_{\rm C} \lesssim 0.34\,M_\odot$, consistent with the constraints inferred dynamically and from eclipse modeling (§4.2).

4.3.2. A Bloated Companion

The companion does not necessarily have to be on the main sequence. Indeed, bloating might be expected: most formation mechanisms produce a binary that has substantial eccentricity initially, and the amount of energy that needs to be dissipated in order to circularize the orbit is a substantial fraction of the binding energy of a low-mass star[9] (Verbunt 1994). Bloating may also be required, as alluded to in § 1 and discussed in § 5, for tidal dissipation to have circularized the orbit in the short time since formation.

We are not aware of detailed calculations of bloating due to tidal dissipation for almost completely con-

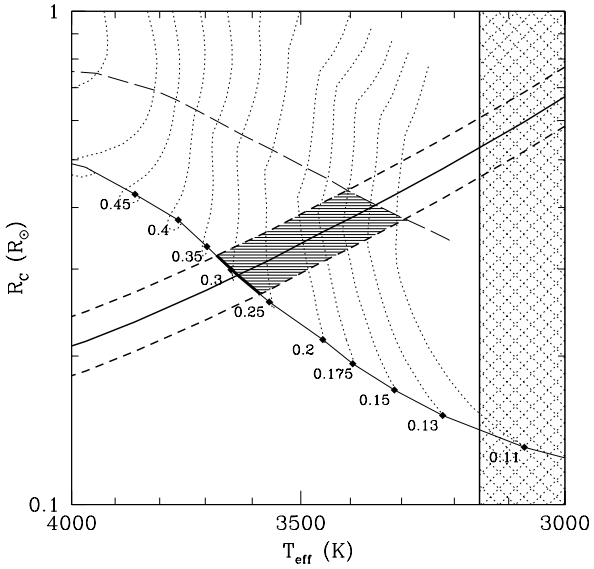

Fig. 2.— Constraints on the radius and temperature of the companion of PSR B1718−19. The continuous curve with dashed curves next to it indicates the constraint set by our measured F702W magnitude. The bold vertical line with the hashed region to the right indicates the limit to the temperature set by the limit to the $m_{\rm F702W} - I$ color. The continuous curve labeled with masses (in solar units) indicates the relation expected for main sequence stars with [Fe/H] = −0.5; the bold section of this curve represents the allowed range if the star is on the main sequence (§4.3.1). As argued in the text, the companion may have become bloated due to irradiation or tidal dissipation. The dotted lines indicate pre-main-sequence tracks for various masses. These are close to the Hayashi limit, and stars in hydrostatic equilibrium can only be on or to the left of these tracks. The long-dashed curve connects the maximum (Roche) radii the companion could have if it were on such a track. The shaded region shows the full range of allowed parameters (§ 4.3.2).

[9]The star cannot be large because of having evolved off the main-sequence, as a star at or past the turn-off mass would have a luminosity much higher than the limit implied by our observations. Even if mass were lost, the thermal timescale for such a star likely is too long for the luminosity to have changed substantially.

vective, low-mass stars[10]. Regardless of the expansion process, however, for a given mass an upper limit to the radius is set by the Roche radius, above which mass transfer would occur. Furthermore, for given mass and radius, a lower limit to the temperature is set by the Hayashi (1961) limit, below which a star cannot be in hydrostatic equilibrium.

To delineate the constraint on the temperature, we can use pre-main-sequence tracks, since these follow the Hayashi limit closely. Indeed, it seems not unlikely that the companion is currently contracting along a similar track, since all processes that could have induced bloating (irradiation, tidal heating) should have ceased to be operative (the pulsar's spin-down luminosity being very low and tidal dissipation having ceased as the orbit became circular). Of course, it is not clear that there has been enough time for the companion to adapt to a quasi–pre main sequence configuration. On the other hand, if the bloating is due to tidal heating, and if the energy was dissipated somewhere in the convective regions, convection would have distributed the energy throughout the star and expansion may well have been along a quasi–pre main sequence track as well.

In Fig. 2, dotted lines indicate the pre-main-sequence tracks of Baraffe et al. (1998), and the long-dashed line shows the Roche radii for the whole range of masses. Under our assumptions, the companion must lie between the latter line and the main sequence, and at any given radius and temperature, an upper limit to its mass is set by the mass for which the pre-main-sequence track passes through that radius and temperatures. In addition, it must reproduce the observed F702W flux and be consistent with the $m_{\rm F702W} - I$ limit. The allowed ranges are $3300 \lesssim T_{\rm eff} \lesssim 3680\,{\rm K}$ and $0.44 \gtrsim R_{\rm C} \gtrsim 0.26\,R_\odot$. The inferred masses are $0.11 \lesssim M_{\rm C} \lesssim 0.34\,M_\odot$, consistent with the constraints inferred dynamically and from eclipse modeling (§4.2) except for the very low-mass end ($M_{\rm C} \lesssim 0.12\,M_\odot$), at which total eclipses would be expected (for a $1.35\,M_\odot$ neutron star), which are not observed.

5. Discussion

We now discuss the implications of our results. The assumption we continue to make is that the system is associated with NGC 6342 and that we have detected the counterpart. The constraints we regard as most important are: (i) the system was brought to its present state $\lesssim 10\,{\rm Myr}$ ago; (ii) the current orbit is nearly circular ($e \lesssim 0.005$); and (iii) the companion has $0.26 \lesssim R_{\rm C} \lesssim 0.44\,R_\odot$ and $3680 \gtrsim T_{\rm eff} \gtrsim 3300\,{\rm K}$. In these ranges, the left-hand limits correspond to the case where the companion is a $\sim 0.3\,M_\odot$ main-sequence star, while the right-hand limits correspond to the case where the companion is a $\sim 0.13\,M_\odot$ star which has been maximally bloated and is currently contracting along a pre-main-sequence track.

Below, we first briefly review the formation models that have been suggested, in order to set the stage for a discussion of how the system could have been circularized. We end by noting briefly what constraints one could set if the star we detected is not the counterpart of PSR B1718−19, or if the system is not in NGC 6342.

5.1. Formation Models

Two models have been suggested to explain the origin of the PSR B1718−19 system. One is that the neutron star was formed early in the life of the globular cluster (Lyne et al. 1993; Wijers & Paczynski 1993; Zwitter 1993; Ergma et al. 1996). It had stopped being a radio pulsar and was dormant until it had a close interaction with a star or binary, $\sim 10\,{\rm Myr}$ ago. During that interaction, some mass was lost from a normal star, part of which was accreted by the neutron star. As a consequence, it was spun up sufficiently for the radio mechanism to become active again, yet did not undergo a long phase of mass transfer and thus kept a large magnetic field. Similar close encounters have been invoked to explain the presence of two other long-period (but single) pulsars in globular clusters: PSR B1745−20 in NGC 6440 and PSR B1820−30B in NGC 6624 (Lyne, Manchester, & D'Amico 1996).

To give the system the velocity required by the present location far outside the cluster core and conserve momentum, the putative interaction must have involved at least one other object. The system's initial orbit is expected to have been highly eccentric, $e \gtrsim 0.8$ (see, e.g, Phinney 1992).

The second model that has been considered for the origin of the PSR B1718−19 system is that the neutron star was formed via accretion-induced collapse (AIC) of a white dwarf (Lyne et al. 1993; Ergma 1993; Wijers & Paczynski 1993; Ergma et al. 1996). The kick imparted to the neutron star during AIC,

[10] See Podsiadlowski (1996) for calculations for somewhat more massive stars, for which only the outer layers are convective.

whether intrinsic or due to mass loss, must have been relatively small, since otherwise the systemic velocity would have been so large that the system would have left the cluster long ago. For a kick of order the $20\,\mathrm{km\,s^{-1}}$ escape velocity from the core (Webbink 1985), an initial eccentricity of ~ 0.2 is expected.

Given such a kick, the increase in the orbital separation should have been small, about a factor 1.25. Thus, the companion, which must have filled its Roche lobe before AIC for mass transfer to occur, should still be close to filling its Roche lobe. This implies that it cannot have been a Roche-lobe filling main-sequence star, as this would require a mass of $\sim 0.7\,M_\odot$ and hence a much brighter optical counterpart than we observe (see Fig. 2). It has been suggested that the star was bloated already before AIC due to irradiation from the primary during the mass transfer phase (Ergma 1993; Ergma et al. 1996). It is not clear whether strong bloating is possible by irradiating only one side of a star (e.g., King et al. 1996), but if it happened, the star should still be bloated, because the thermal time scale is much longer than the pulsar characteristic age.

5.2. Circularization

In both formation scenarios that have been suggested, the initial binary orbit is expected to be eccentric. Indeed, in general any event that imparted a systemic velocity large enough for the system to (almost) escape the cluster will most likely have left the binary orbit eccentric. The current tiny eccentricity therefore requires explanation. Since eccentricity likely decays exponentially, the current low e, even for an initial eccentricity as small as $e \simeq 0.1$, requires a circularization time $t_{\rm circ} \lesssim \tau_{\rm sd}/4 = 2.5\,\mathrm{Myr}$.

It is not straightforward to estimate whether such a short $t_{\rm circ}$ is possible. This is because the companion is probably completely convective, with convective turnover time scales far longer than the 6.2-h orbital period (see below). This makes the energy transfer less efficient, and thus circularization time scales longer, but it is not clear to what extent. We will first use the prescription of Zahn (1989), in which the efficiency is assumed to decrease linearly with the ratio of the convective to orbital timescale, and then discuss the prescription of Goldreich & Nicholson (1977) and Goodman & Oh (1997), in which the efficiency decreases almost quadratically with the timescale ratio. We should stress that at present it is not clear that either prescription is reliable; see Goodman & Oh for a discussion.

Following the formalism of Zahn (1989; Eq. [21]), we write[11]

$$\frac{1}{t_{\rm circ}} = -\frac{1}{e}\frac{{\rm d}e}{{\rm d}t} = 21\frac{\lambda_{\rm circ}}{t_{\rm f}} q(1+q)\left(\frac{R_{\rm C}}{a}\right)^8, \qquad (1)$$

where $t_{\rm circ}$ is the circularization timescale, e the eccentricity, $\lambda_{\rm circ}$ a dimensionless average of the turbulent viscosity weighted by the square of the tidal shear, $t_{\rm f} = (M_{\rm C}R_{\rm C}^2/L_{\rm C})^{1/3}$ the convective friction time, $q = M_{\rm PSR}/M_{\rm C}$ the mass ratio, and a the orbital separation. Here, all uncertainty is hidden in the parameter $\lambda_{\rm circ}$. In the prescription of Zahn (1989), it can be approximated by $\lambda_{\rm circ} \simeq 0.019\alpha^{4/3}(1+\eta^2/320)^{-1/2}$, where α is the mixing length parameter and $\eta = 2t_{\rm f}/P_{\rm orb}$ a measure of the timescale mismatch.

For a main-sequence star companion with parameters in the ranges listed above, we find $t_{\rm f} \simeq 0.5\,\mathrm{yr}$ and $\eta \simeq 1500$. Assuming $M_{\rm PSR} = 1.4\,M_\odot$ (i.e., $a \simeq 2\,R_\odot$) and taking $\alpha = 2$ (as in Zahn [1989]; consistent with the observational constraint derived by Verbunt & Phinney [1995] for small η), one infers $\lambda_{\rm circ} \simeq 6\times10^{-4}$, and a circularization time in the range $5 \lesssim t_{\rm circ} \lesssim 17\,\mathrm{Myr}$, too long to understand the current small eccentricity. If the star is bloated, circularization is much faster, because of the very strong dependence on the ratio $R_{\rm C}/a$: we find $t_{\rm circ} \simeq 0.07\,\mathrm{Myr}$ for a maximally bloated companion.

The situation is different for the prescription of Goodman & Oh (1997), in which $\lambda_{\rm circ} \propto \eta^{-2}$. Extrapolating in their Fig. 2, we infer $\lambda_{\rm circ} \simeq 4\times10^{-6}$ (note their slightly different definition of η). Thus, the inferred circularization times are two orders of magnitude longer than those estimated with the prescription of Zahn (1989); if correct, it may be difficult to understand how the orbit could have been circularized even if the companion was maximally bloated.

As mentioned in § 4, the star could have become bloated due to the energy dissipated by the circularization proper (Verbunt 1994). It is difficult to estimate, however, by how much, as it is not clear where, how, and on what time scale the tidal energy is dissipated, especially in such a low-mass star. For high eccentricity, the tides excite low-order pulsation modes in the star, which will be dissipated, either by direct viscous damping (Kochanek 1992), or, perhaps more likely, by non-linear coupling to higher-degree modes and damping of these (Kumar & Goodman

[11] See Phinney (1992) for a pedestrian derivation.

1996). For either case, it appears that for a low-mass, (almost) completely convective star ($\lesssim 0.5 M_\odot$), most of the energy will be dumped in the outermost layers. These will be heated and may expand, which would lead to stronger tidal coupling.

If the expansion involved the whole star, or a substantial fraction of it, most likely the star would still be bloated, as the thermal time would be much longer than the pulsar characteristic age. Also if only the outer layers of the star expanded, however, it seems likely the star would still be bloated, as otherwise it would be difficult to reduce the eccentricity sufficiently. This is because the tidal luminosity will decrease rapidly with decreasing eccentricity and increasing periastron distance; if the expanded layers shrunk too quickly in response, the circularization time would have become long again while the eccentricity was still substantial. One way to verify whether the companion is still bloated is to measure its temperature.

5.3. Caveat: Fainter Companion

There is a probability of about one in five of a chance coincidence between PSR B1718−19 and the object in our HST images (§ 3). If so, the companion has to be substantially fainter, with $m_{\rm F702W} > 27.2$ (§ 3). One can go through a similar exercise as in § 4.3 to constrain the companion properties for this case. The result is that the companion needs to have mass $\lesssim 0.15\,M_\odot$, close to the minimum allowed by pulse timing. In this case, the circularization time scale problem is exacerbated.

Another possibility is that PSR B1718−19 is not associated with NGC 6342. Indeed, the dispersion measure is only $71\,{\rm cm}^{-3}\,{\rm pc}$, while $130\,{\rm cm}^{-3}\,{\rm pc}$ is expected for NGC 6342 (Taylor & Cordes 1993). Taken at face value, a distance of only 3 kpc is implied. If PSR B1718−19 were in the foreground, again the companion would be less luminous and thus less massive, even more problematic for circularization.

6. Conclusions

In summary, using HST observations, we have detected a faint star at the position of the unusual eclipsing binary radio pulsar PSR B1718−19. This faint star most likely is the pulsar's companion. We have shown that it is difficult to explain the highly circular present-day orbit if the companion is a $M_{\rm C} \simeq 0.3\,M_\odot$, $R_{\rm C} \simeq 0.3\,R_\odot$ main-sequence star (unless circularization was not by tidal interaction). If it is a bloated, $R_{\rm C} \gtrsim 0.4\,R_\odot$ star, circularization may be sufficiently rapid, depending on the extent to which the efficiency of tidal dissipation is suppressed by the orbital period being far shorter than the convective turnover time in the star. The system thus provides an interesting test-case for tidal-interaction theory.

A measurement of the color of the companion would be the best way to determine whether it is bloated or not. For a main-sequence star with $T_{\rm eff} = 3640\,{\rm K}$ and a bloated star with $T_{\rm eff} = 3300\,{\rm K}$, one expects $(R-I, I-J, J-H, H-K)_0 = (1.0, 1.1, 0.6, 0.2)$ and $(1.3, 1.4, 0.6, 0.2)$, respectively. Radio and optical proper-motion studies could settle association of our candidate counterpart with PSR B1718−19, and of the system with NGC 6342.

We are indebted to the referee, R. Webbink, for his thoughtful report, and, in particular, for pointing out the importance of the Hayashi limit for constraining the temperature of a bloated companion. We also thank him for the estimate of the relaxation time of PSR B1718−19 at its present position in NGC 6342. We thank M. Goss for help with the VLA observations, and P. Goldreich, V. Kalogera, F. Rasio, S. Sigurdsson, C. Tout, M. van den Berg, F. Verbunt, and R. Wijers for useful discussions. The observations were obtained at the W. M. Keck Observatory on Mauna Kea, Hawaii, which is operated by the California Association for Research in Astronomy, and with the NASA/ESA Hubble Space Telescope at STScI, which is operated by AURA. The reduction of the optical data was done using the Munich Image Data Analysis System (MIDAS), which is developed and maintained by the European Southern Observatory. This research made use of the SIMBAD data base. We acknowledge support of a NASA Guest Observer grant (GO-06769.01-95A), a fellowship of the Royal Netherlands Academy of Arts and Sciences (MHvK), a NSF grant (95-30632; ARK), a Sloan Research Fellowship (VMK), and visitor grants of the Netherlands Organisation for Scientific Research NWO (VMK) and the Leids Kerkhoven-Bosscha Fonds (MHvK, VMK). MHvK thanks MIT and Caltech for hospitality, VMK the Aspen Center for Physics and Utrecht University.

REFERENCES

Baggett, S., Casertano, S., Gonzaga, S., & Ritchie, C., 1997, WFPC2 Instrument Science Report

97-10 (Baltimore: STScI)
Baraffe, I., Chabrier, G., Allard, F., Hauschildt, P. H. 1998, A&A, 337, 403
Burderi, L., & King, A. R. 1994, ApJ, 430, L57
Chaboyer, B., Demarque, P., Kernan, P. J., & Krauss, L. M. 1998, ApJ, 494, 96
Ergma, E. 1993, A&A, 273, L38
Ergma, E., Sarna, M. J., & Giersz, M. 1996, A&A, 307, 768
ESA 1997, The Hipparcos and Tycho Catalogues, ESA SP-1200
Goldreich, P., & Nicholson, P. D. 1977, Icarus, 30, 301
Goodman, J., & Oh, S. P. 1997, ApJ, 486, 403
Harris, W. E. 1996, AJ, 112, 1487
Hayashi, C. 1961, PASJ, 13, 450
Holtzman, J. A., et al. 1995a, PASP, 107, 156
Holtzman, J. A., Burrows, C. J., Casertano, S., Hester, J. J., Trauger, J. T., Watson, A. M., & Worthey, G. 1995b, PASP, 107, 1065
King, A. R., Frank, J., Kolb, U., & Ritter, H. 1996, ApJ, 467, 761
Kochanek, C. 1992, ApJ, 385, 604
Kumar, P., & Goodman, J. 1996, ApJ, 466, 946
Lyne, A. G., Biggs, J. D., Harrison, P. A., & Bailes, M. 1993, Nature, 361, 47
Lyne, A. G., Manchester, R. N., & D'Amico, N. 1996, ApJ, 460, L41
Mathis, J. S. 1990, ARA&A 28, 37
Oke, J. B., et al. 1995, PASP, 107, 375
Phinney, E. S. 1992, Phil. Trans. R. Soc. Lond. A, 341, 39
Podsiadlowski, P. 1996, MNRAS, 279, 1104
Salaris, M., & Weiss, A. 1998, A&A, 335, 953
Taylor, J. H., & Cordes, J. M. 1993, ApJ, 411, 674
Thorsett, S. E. 1995, in Millisecond Pulsars: A Decade of Surprise, eds. A. S. Fruchter, M. Tavani, & D. C. Backer, ASP Conf. Ser. 72, 253
Thorsett, S. E., & Chakrabarty, D. 1999, ApJ, 512, 299
Urban, S. E., Corbin, T. E., Wycoff, G. L., Martin, J. C., Jackson, E. S., Zacharias, M. I. & Hall, D. M. 1998a, AJ, 115, 1212
Urban, S. E., Corbin, T. E., & Wycoff, G. L. 1998b, AJ, 115, 2161
van den Heuvel, E. P. J. 1995, J. Astrophys. Astron., 16, 255
Verbunt, F. 1994, A&A, 285, L21
Verbunt, F., & Phinney, E. S. 1995, A&A, 296, 709
Webbink, R. F. 1985, in IAU Symp. 113, Dynamics of Stellar Clusters, ed. J. Goodman & P. Hut (Dordrecht: Kluwer), 541
Wijers, R. A. M. J. & Paczynski, B. 1993, ApJ, 415, L115
Zahn, J.-P. 1989, A&A, 220, 112
Zwitter, T. 1993, MNRAS, 264, L3

This 2-column preprint was prepared with the AAS LaTeX macros v4.0.